AN INTRODUCTION TO SCALING VIOLATIONS

G. PARISI
Laboratori Nazionali di Frascati
Frascati (Italy)

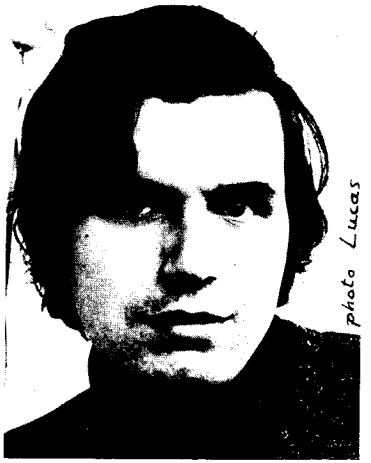

Abstract: The theory of scaling violations in deep inelastic scattering is presented using the parton model language; intuitive physical arguments are used as far as possible. In the comparison between theory and experiments particular attention is payed to the consequences of the opening of the threshold for charm production.

Resumé : On utilise ici le language du modèle a partons pour exposer la théorie de la violation de la loi d'échelle dans la diffusion très inélastique, en employant autant que possible des argumenta intuitifs. On compare ensuite théorie et donnés expérimentales en étudiant avec attention particulière les conséquences de l'overture du seuil pour produire du charm.

1. - INTRODUCTION(x)

ὅσων ὄψις ἀκοὴ μάθησις, ταῦτα ἐγὼ προτιμέω (o)
(Heracleitus)

I think that deep inelastic scattering is one of the best processes which can be used to test our theoretical understanding of strong interactions. The success of the Bjorken scaling law and the ability of the parton model to explain the experimental data are the main historical motivations for our present belief in the quark model.

It has now been realized that the naive quark-parton model is inconsistent and that small violations of the scaling law must be present: more accurate data seem to agree with this conclusion. The standard theoretical arguments which are used to study scaling violations are mainly based on sophisticated field theory techniques such as Wilson expansion at short distances and on the light cone, anomalous dimensions, bilocal operators.... All this theoretical machinery has been essential to derive unambigous and correct results, however we have departed from the physically intuitive approach which makes the standard parton model so appealing.

In this introduction to the violations of the scaling law, we try to recover the physical interpretation of the theory; to this end the language of the parton model will be used to derive and interpret the theoretical results. We hope that this paper will partially fill the gap between the conclusions of the parton model (which are physically motivated but incorrect) and the conclusions of a field theoretical analysis (which are correct but whose intuitive interpretation has been lost somewhere(+).

2. - THE PARTON MODEL

Let us briefly review the main ideas which are behind the parton model[6] in order to understand how they must be modified to account for the violations of the Bjorken scaling law.

(x) - Part of the results presented here have been obtained by the author in collaboration with G. Altarelli and R. Petronzio[1-3].

(o) - The things of which there is seeing and hearing and perception, these do I prefer.

(+) - This point of view is not new: a similar approach has been advocated by Polyakov[4] and by Kogut and Susskind[5].

In a deep inelastic process an highly virtual photon of mass Q^2 interacts with the pointlike constituents (partons) of the hadron. In the Breit frame the photon carries no energy and the proton has a momentum P proportional to $(Q^2)^{1/2}$. For high Q^2, P is large and the proton looks like a highly Lorentz contracted pancake; the time (τ) of interaction is proportional to $(Q^2)^{-1/2}$. For small τ we can safely suppose that the photon scatters incoherently on each parton; the cross section for deep inelastic scattering depends on the parton distribution seen when we look inside the hadron with a resolution time τ.

The cross section for longitudinaly (σ_L) and transverse (σ_T) polarized photons can be written using two independent structure functions[7]: $F_1(x, Q^2)$, $F_2(x, Q^2)$, x being equal to $2M\nu/Q^2$.

For spin 1/2 partons:

$$F_2(x, Q^2) = \Sigma_i e_i^2 \, x N_i(x, \tau) , \qquad \tau = (Q^2)^{-1/2} , \tag{2.1}$$

where $N_i(x, \tau)$ is the number of partons of the i-th type, having charge e_i and carrying longitudinal momentum xP; σ_L/σ_T is proportional to $\langle p_\perp^2 \rangle / Q^2$, where $\langle p_\perp^2 \rangle$ is the mean squared value of the transverse momentum carried by the partons.

This is quite general: we have only assumed that the electromagnetic current couples to point-like constituents and that the final state interaction does not change total cross sections at very high energies: after the interaction with the photon the system evolves in time with its own hamiltonian.

The Bjorken scaling law follows from the assumption that:

$$\lim_{\tau \to 0} N(x, \tau) = N(x) \neq 0 . \tag{2.2}$$

In very short times partons cannot modify their distribution inside the hadron: they move slowly and they can be considered free on a short time scale.

Two main assumptions are thus involved in the derivation of the Bjorken scaling law:

a) The hadron interacts with an highly virtual photon via some point-like constituents (partons). Final state interactions can be neglected.

b) The constituents cannot change their momentum too fast: their interactions can be neglected in the limit $\tau \to 0$.

However what is the rationale for these assumptions? In any reasonable quantum field theory in 4 dimensional space-time the first one is valid, the second one is false[8-9].

For example in quantum electrodynamics the validity of both assumptions would imply that the radiative corrections scale with the energy and are the same both for $e\bar{e}$ and $\mu\bar{\mu}$ scattering. Anyone working in high energy physics knows that this is not the case and that radiative corrections show a logaritmic dependence on E/m.

If the first hypothesis is true, even in presence of scaling violations the parton model inequalities in deep inelastic scattering (e.g. $1/4 \leq \leq F_2^n(x,Q^2)/F_2^p(x,Q^2) \leq 4$) are unchanged. The failure of the second hypothesis implies that the Bjorken scaling law is no more valid and that more complicated scaling laws are satisfied. These new scaling laws depend on the detailed dynamics of the strong interactions and their verification would be quite important.

Before discussing what happens in the strong interaction case, I want to clear up the situation in a more familiar case, i.e. quantum electrodynamics. This will be done in sections 3 and 4. In section 5 I will present the theoretical results based on a coloured gauge theory of strong interactions. In sections 6 and 7 I will compare the theoretical results with the experimental data on electron and neutrino scattering.

3. - THE COSTITUENTS OF THE ELECTRON

ἐν δὲ μέρει κρατέουσυ περυπλομένοιο κύκλοιο, καὶ φθίνει εἰς ἄλληλα καὶ αὔξεται ἐν μέρει αἴσης (x)

(Empedocles)

Pure quantum electrodynamics is a good place to study the violations of the Bjorken scaling law. They show up in very simple and familiar formulae: the equivalent number of photons in an electron on energy E (momentum P = E) is:

$$N_\gamma(x,P) \simeq \frac{\alpha}{2\pi}\frac{4}{x}\ln(P/m_e) + O(\alpha^2) , \qquad (3.1)$$

(x) - In turn they (elements) get the upper hand in the revolving cycle, and perish into one another and increase in the turn appointed by their fate.

where x is the fraction of longitudinal momentum carried by the photon. If we interpret $1/P \simeq (1/Q^2)^{1/2}$ as the resolution time τ, we obtain that the equivalent number of photons in the electron is :

$$N_\gamma(x,\tau) = \frac{\alpha}{2\pi}\frac{4}{x}\ln(1/m_e\tau) + O(\alpha^2) \quad , \quad \tau m_e \ll 1 . \tag{3.2}$$

This quantity goes to infinity when $\tau \to 0$ and the assumption b) (eq. 2.2) of the last section is violated. Moreover for each photon of momentum xP there must be an electron of momentum $(1-x)P$; the momentum distribution of the electrons inside the electron is :

$$N_e(x,\tau) = \delta(x-1) + \frac{\alpha}{2\pi}\left[\frac{4}{1-x} - 2C\,\delta(x-1)\right]\ln(1/m_e\tau) . \tag{3.3}$$

The constant C is fixed by the condition that the total number of electrons is not changed by the interaction :

$$\int_0^1 N_e(x,\tau)\,dx = 1 . \tag{3.4}$$

Stricly speaking C is logaritmically divergent ($C = 2\int_0^1 \frac{dx}{1-x}$). The two divergences in eq. (3.4) cancel each other.

However eqs. (3.1) and (3.3) cannot be used directly to study the limit $\tau \to 0$: the neglected higher order terms become important when $\alpha \ln \tau \simeq 1$. Let us first study the effect of multiple photon emission (see Fig. 1). The key step is to concentrate one's attention on the time derivative of the number of electrons ; the variable $L = -2\ln(m_e\tau)$ is introduced for convenience.

From eq. (3.3) we find :

$$\frac{dN_e(x,L)}{dL} = -\frac{1}{2}\frac{dN_e(x,\tau)}{d\ln\tau} = \frac{\alpha}{2\pi}\frac{2}{1-x} - C\,\delta(x-1) = \frac{\alpha}{2\pi}P_{ee}(x) . \tag{3.5}$$

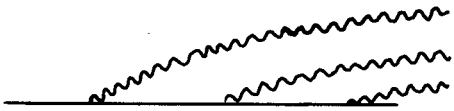

fig.1

FIG. 1 -A typical diagram contributing to multiple photon emission.

Eq. (3.5) suggests that the transition probability for electron bremsstrahlung is independent of L. However the electron distribution is L dependent: the change in time of the electron distribution must be the product of the transition probability p and the actual electron distribution at "time" L. One is led to the following "master" equation:

$$(3.6) \qquad \frac{dN_e(x,L)}{dL} = \frac{\alpha}{2\pi}\int_x^1 \frac{dy}{y} N_e(y,L)\, p_{ee}(x/y) =$$

$$= \frac{\alpha}{2\pi}\left[-CN_e(x,L) + \int_x^1 N_e(y,L)/(y-x)\, dy\right].$$

The first term arises from the decrease of $N_e(x,L)$ due to the bremsstrahlung of electrons staying at the point x: it is naturally proportional to $N_e(x,L)$. The second term represents the increase in the number of electrons at the point x due to bremsstrahlung of electrons carrying momentum $y > x$, the relative loss of electron momentum being x/y.

Eq. (3.6) can be easily solved by computer; qualitative statements can be made studying the L dependence of the moments:

$$(3.7) \qquad M_e^N(L) = \int_0^1 \frac{dx}{x} x^N N_e(x,L).$$

Substituting eq. (3.6) in the derivative of eq. (3.7) we obtain:

$$(3.8) \qquad \frac{dM_e^N(L)}{dL} = \frac{\alpha}{2\pi}\int_0^1 \frac{dx}{x} x^N N_e(x,L) \int_0^1 \frac{dy}{y} y^N p_{ee}(y) =$$

$$= -\frac{\alpha}{2\pi} M_e^N A_{ee}^N; \qquad A_{ee}^1 = 0 \qquad A_{ee}^N > 0 \ (N > 1),$$

whose solution is:

$$(3.9) \qquad M_e^N(L) = M_e^N(L_o)\exp\left[-\frac{\alpha}{2\pi} A_{ee}^N (L-L_o)\right].$$

M^1 is the total number of electrons in the system and it is a constant. M^2 is the total momentum in P units carried by the electrons and it goes exponentially to zero: the whole momentum is transferred from the electron to the photon system. Increasing L, $N_e(x,L)$ shifts towards $x = 0$ and asymptotically it is concentrated at this point.

Eqs. (3.6-3.9) are valid in the so called leading logaritm approximation (terms proportional to $(\alpha L)^n$ are retained and terms proportional to $\alpha(\alpha L)^n$ are neglected).

The transition probabilities p_{ee} contain higher orders in α; however these new terms are not L dependent and no qualitative conclusion is changed; to neglect them is a good approximation for all values of L if α is not too large.

A similar equation can be written for the photons:

$$\frac{dN_\gamma(x, L)}{dL} = \frac{\alpha}{2\pi} \int_x^1 \frac{dy}{y} N_e(y, L)\, p_{\gamma e}(x/y) . \tag{3.10}$$

The following relation holds:

$$p_{\gamma e}(x) = p_{ee}(1-x) . \tag{3.11}$$

However the situation is not so simple: the photon itself may split in a $e\bar{e}$ pair, each of the new born e or $\bar{e}$ may emit a photon and so on. The whole process is quite similar to the evolution of an electromagnetic shower in lead. A typical diagram is shown in Fig. 2.

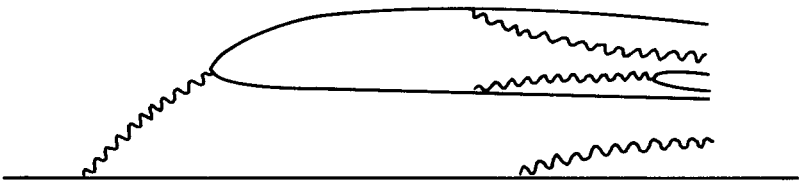

fig.2

FIG. 2 - A typical diagram contributing to the formation of the "shower".

It is clear that we must introduce in the game the distributions of the e, $\bar{e}$ and γ inside the electron; using the same arguments as in the previous case a more complicated master equation can be derived:

$$\frac{dN_e(x, L)}{dL} = \frac{\alpha}{2\pi} \int_x^1 \frac{dy}{y} \left[N_e(y, L)\, p_{ee}(x/y) + N_\gamma(y, L)\, p_{e\gamma}(x/y) \right] ,$$

$$\frac{dN_{\bar{e}}(x, L)}{dL} = \frac{\alpha}{2\pi} \int_x^1 \frac{dy}{y} \left[N_{\bar{e}}(y, L)\, p_{\bar{e}\bar{e}}(x/y) + N_\gamma(y, L)\, p_{\bar{e}\gamma}(x/y) \right] , \tag{3.12}$$

$$\frac{dN_\gamma(x,L)}{dL} = \frac{\alpha}{2\pi}\int_x^1 \frac{dy}{y}\left\{ N_\gamma(y,L)p_{\gamma\gamma}(x/y) + \right.$$
$$\left. + \left[N_e(y,L) + N_{\bar{e}}(y,L)\right] p_{\gamma e}(x/y)\right\} ,$$

where:

$$p_{ee}(y) = p_{\bar{e}\bar{e}}(y) = p_{\gamma e}(1-y) = p_{\gamma\bar{e}}(1-y) ,$$

$$p_{\bar{e}\gamma}(y) = p_{e\gamma}(y) = p_{e\gamma}(1-y) = \frac{1}{2}\left[y^2 + (1-y)^2\right] ,$$

(3. 13)

$$p_{\gamma\gamma}(y) = - C_\gamma \delta(y-1) ,$$

$$C_\gamma = \frac{1}{2}\int dy \left[p_{e\gamma}(y) + p_{\bar{e}\gamma}(y)\right] = \frac{1}{3} .$$

The meaning of these equations is quite clear. The last equation implies that the number of photons which disappear at the point x it is equal to the number of new born $e\bar{e}$ pairs carrying total momentum x. The functions $p_{e\gamma}$ and $p_{\gamma e}$ are related to the longitudinal distributions of bremsstrahlung photons and of Dalitz pair electrons(x).

It is interesting to note that the derivative of the difference of the number of electrons and positrons does not depend on the γ distribution:

(3. 14)
$$\Delta N(x,L) = N_e(x,L) - N_{\bar{e}}(x,L) ,$$

$$\frac{d\Delta N(x,L)}{dL} = \int_x^1 \frac{dy}{y}\Delta N(y,L)\, p_{ee}(x/y) .$$

The L evolution of this difference decouples from that of the other functions. Also this coupled set of equations can be easily solved with a computer: the knowledge of the three functions N_e, $N_{\bar{e}}$ and N_γ at a particular value of L in the region $1 > x > x_m$ allows us to compute them at any value of L, in the same x region.

It is possible to study the behaviour of the moments of the distributions; if one defines a three component vector

---

(x) - The possibility of using these formulae to compute higher order processes in quantum electrodynamics has been suggested by Cabibbo. This technique has been applied to the study of the reactions $e^+e^- \to e^+e^-$ (10) and $e^+e^- \to e^+e^-e^+e^-$ (11).

(3.15) $$M_i^N(L) = \int_0^1 \frac{dx}{x} x^N N_i(x,L)$$ $i = 1 \leftrightarrow e$, $i = 2 \leftrightarrow \bar{e}$, $i = 3 \leftrightarrow \gamma$

one finds :

(3.16) $$\frac{dM_i^N(L)}{dL} = -\frac{\alpha}{2\pi} A_{iK}^N M_K^N(L) ,$$

where A is a three by three matrix. If we denote by λ_a^N and $\vec{u}_a^N$ the three eigenvalues and eigenvectors of A^N, the solution of (3.16) can be written using the vectorial notations as :

(3.17) $$\vec{M}^N(L) = \sum_1^3 a\, M_a^N \vec{u}_a^N \exp -\frac{\alpha}{2\pi}(L-L_o)\lambda_a^N .$$

The quantities M_a^N are fixed by the boundary condition $\vec{M}^N(L)\big|_{L=L_o} = \vec{M}^N(L_o)$.

For N = 2 one of the eigenvalues is 0, reflecting the conservation of the total momentum carried by the constituents. When $L \to \infty$ the distributions of both electrons and photons shifts towards 0, the ratio of the momentum carried by the electrons and the positrons goes to one and the total momentum carried by the "valence" electron goes to zero, while the momentum carried by the sea of $e\bar{e}$ pairs and by the photons goes to a constant. In the limit $L \to \infty$ an equilibrium situation is reached : the momentum lost by the electrons via bremsstrahlung is equal to the momentum refilling due to the creation of Dalitz pairs. The mean value of the momentum carried by each constituent goes to zero and this degradation of momentum is the origin of the progressive concentration of the functions N(x, L) near x = 0. Up to now, we have considered only the distributions in longitudinal momentum. The transverse momentum distribution can be studied using similar techniques ; one finds[12] :

$$\frac{\sigma_L}{\sigma_T} \propto \frac{\langle p_\perp^2 \rangle}{p^2} = \bullet(\alpha) .$$

Unfortunately the situation is not so simple : we have neglected the possibility that an $e\bar{e}$ pair annihilate in a photon which subsequently splits in an $e\bar{e}$ pair and so on. A typical diagram is shown in Fig. 3.

To study this phenomenum a new concept must be introduced : vacuum polarization. The effect of these new diagrams can be accounted for, by the introduction of an effective L dependent coupling constant.

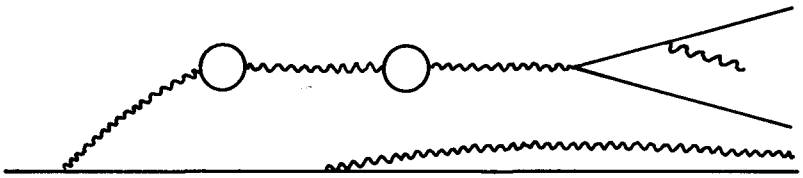

fig.3

FIG. 3 -A typical diagram contributing to vacuum polarization.

We prefer to discuss the consequences of vacuum polarization and to write the final formulae in this section; we postpone to the next section the discussion on the rationale and on the physical meaning for the introduction of an effective time dependent coupling constant. The correct formulae are obtained by substituting α by $\alpha(L)$ in eqs. 3.12 and 3.16. The function $\alpha(L)$ satisfies the differential equation:

$$\frac{d\alpha(L)}{dL} = \beta\alpha^2(L) + \bullet\left[\alpha^3(L)\right] , \qquad L \gg 1 , \tag{3.18}$$

whose solution is:

$$\alpha(L) = \frac{\alpha(L_0)}{1 - \beta(L-L_0)\alpha(L_0)} , \qquad \alpha(L),\ \alpha(L_0) \ll 1 . \tag{3.19}$$

Two different possibilities are open[13]:

a) $\beta > 0$,

b) $\beta < 0$.

In case a) the effective coupling increases with L, also if we start from a small value of α, increasing L we are projected in the strong coupling regime where we cannot justify our approximation of neglecting higher order in α in the transition probabilities p. What will finally happen in this case is still an open problem: no general consensus has been reached on this point.

Case a) is realized in pure QED; the energies at which the perturbative expansion become useless are gigantic: they are of the order of the mass of the universe.

Case b) is better understood: increasing L the effective coupling constant decreases; also if we start from a relative large value of α we finally end up with a small value of $\alpha(L)$ ($\alpha(L) \to -1/\beta L$ when $L \to \infty$). In this kind of theory the large L limit can be controlled using a perturba

tive estimate of the transition probabilities, whatever the value of the coupling constant in the low momentum region.

There is no problem to solve the modified eq. (3.12) by computer. Eq. (3.16) becomes now:

$$\frac{dM_i^N(L)}{dL} = -\frac{\alpha(L)}{2\pi} A_{iK}^N M_K^N(L) \quad , \tag{3.20}$$

whose solution is:

$$\vec{M}^N(L) = \sum_1^3 a \, M_a^N \vec{u}_a^N \left[1 - \beta(L-L_o)\alpha(L_o)\right]^{-\frac{\lambda_a^N}{2\pi\beta}} \quad . \tag{3.21}$$

We now have in our hands the tools which are needed to study the violations of the scaling law in deep inelastic scattering. We are able to compute how the distribution of the pointlike constituents depends on the resolution time. We have seen that when the resolution time goes to zero ($L \to \infty$) a continuous process of interchange of momentum among the bare constituents is present, the laws which regulate this phenomenum can be summarized in the "master" equation (3.12).

4. - VACUUM POLARIZATION

It is a common day experience that salt can be easily dissolved in water but not in oil. This fact is due to the high value of the static dielectric constant $\varepsilon_s = 80$ ($\varepsilon_s = 1$ in vaccum). The force between two charges is:

$$F = \frac{q_1 q_2}{\varepsilon_s} \frac{1}{r^2} \quad , \qquad r \to \infty \quad , \tag{4.1}$$

at large distances. However, at distances smaller than the radius of the water molecule (a), one recovers the more familiar:

$$F = q_1 q_2 \frac{1}{r^2} \quad , \qquad r << d \, . \tag{4.2}$$

It is possible to define a function $\varepsilon(r)$ such that:

$$F = \frac{q_1 q_2}{\varepsilon(r)} \frac{1}{r^2} \quad , \qquad \varepsilon(0) = 1 \, , \quad \varepsilon(\infty) = \varepsilon_s \, . \tag{4.3}$$

This effect arises from the orientation of the water dipoles in presence of an electric field. The scale of the phenomenum is naturally given by d.

Equivalently one would define an r dependent effective charge and write:

(4. 4) $$F = q_1(r)\, q_2(r)\, \frac{1}{r^2} \quad , \qquad q_1(r) = q_1 / \sqrt{\varepsilon(r)} \; .$$

A typical plot of q(r) as function of L is shown in Fig. 4.

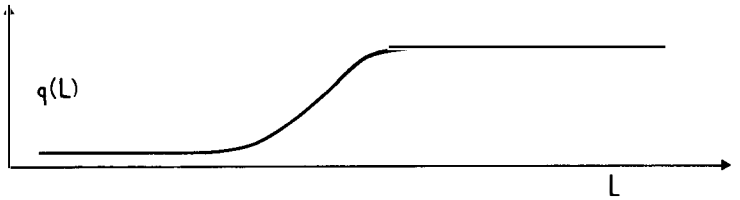

FIG. 4 -The effective charge in water as function of $L = -\ln(r/d)$, r being the distance and d being the radius of water molecules.

The polarization of water decreases the force among Na^+ and Cl^- ions and allows the solution of salt in water: charged ions in water are nearly asymptotically free at large distances while they have a strong interaction at short distances.

A more drammatic effect can be found in metals: here $\varepsilon_s = \infty$ and the effective charge goes to zero exponentially at large distances: the charge is completely shielded.

In quantum electrodynamics the role of water is played by the virtual $e\bar{e}$ pairs which fill the vacuum. The presence of a charge modifies their distribution and produces a polarization of the vacuum which alters the value of the effective charge seen at large distances. The inverse of the mass of the virtual pair corresponds to the radius of water molecules: the shielding effect reaches a constant at distances larger than $1/2\ m_e$. However there is no upper bound to the mass of a virtual pair so that the effective charge changes its value also at very short distances. At distances of order 10^{-100} cm the effective coupling constant becomes of order 1 and non linear phenomena in the electric field are quite important. It is not clear what happens at so short distances, however this problem is not relevant here.

We hope we have clarified why the effective coupling constant in Quantum electrodynamics depends on the distance r and by relativistic invariance also on the resolution time τ. The fact that the force among different (equal) sign charges is attractive (repulsive) implies that in all possible materials, vacuum included, $\varepsilon_s > 1$ and the effective charge at large distances

is smaller than the bare charge: $q(\infty) < q(0)$. We can conceive a world in which the force among charges of the same sign is attractive and among charges of opposite sign is repulsive. We will call the matter of which this world is made up "enantion". The static polarizability of the enantion is always less than 1. Also in this case we can introduce a distance-dependent effective coupling constant: the effective charge seen at large distances is always greater that the bare one:

$$q(\infty) = \frac{q(0)}{\sqrt{\varepsilon_s}} > q(0) \quad . \tag{4.5}$$

Let us chose a particular kind of enantion in which $\varepsilon_s = 0$ and let us suppose that the radius of the molecules has a continous distribution which ranges from zero up to a maximum length d. In this case $q(\infty)/q(0) = \infty$. If the effective charge seen at large distance is finite, the effective charge at very small distance must be equal to zero (see Fig. 5). Two ions in enantion behave as free at short distances while the interaction remains strong at large distances.

Why are we interested in such a devious system? The reason is simple: there are models of strong interactions in which the polarizability properties of vacuum are just the same as those of enantion. These model belong to case b) of section 3 and have a coupling constant which is asymptotically zero at short distance. I think that it is interesting to have a concrete example of a system in which the interaction among pointlike particles fades at short distances.

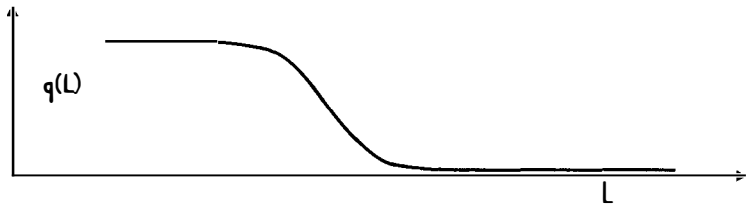

FIG. 5 -The effective charge in enantion as function of $L = -\ln(r/d)$, r being the distance and d being the maximum radius of enantion molecules.

5. - THE STRUCTURE OF STRONG INTERACTIONS

τέσσαρα γὰρ πάντων ῥιζώματα πρῶτον ἄκουε[x]
(Empedocles)

In the most popular model of strong interactions the hadrons are composed of 4 quarks (p, n, λ and p')[14]; the three different colours of quarks interact via the exchange of an octet of coloured gluons. Electromagnetic and week currents are colour singlets; the theory is invariant under the group SU(3) colour.

The effective coupling constant of the theory satisfies the equation[15-17]:

$$\frac{d\alpha(L)}{dL} = -\frac{25}{12\pi}\alpha^2(L) + O(\alpha^3) \qquad (L = \ln Q^2)\,, \tag{5.1}$$

whose solution is:

$$\alpha(L) = \frac{\alpha(L_o)}{1 + \frac{25}{12\pi}(L - L_o)\alpha(L_o)}\,. \tag{5.2}$$

The situation is the same as in enantion. Although the coupling constant of strong interactions is large at distances of order $1/m_\pi$, it is possible that at rather shorter distances it becomes smaller and smaller and that a perturbative approach can be used in the deep inelastic region. If this is the case, it is possible to obtain sharp predictions for the breaking of the Bjorken scaling law for very high Q^2.

We denote by $N_{q_i}(x, L)$ $i = 1, 4$, $N_{\bar{q}_i}(x, L)$ $i = 5, 8$ and $N_g(x, L)$ respectively, the longitudinal momentum distributions of quarks, antiquarks and gluons inside an hadron. The L dependence of these distribution functions can be computed using the transition probabilities for the processes: $q \to q + g$, $g \to q + \bar{q}$ and $g \to g + g$. The first two are present also in quantum electrodynamics, while the third is peculiar to non abelian gauge theories.

The following master equation holds:

$$\frac{dN_{q_i}(x, L)}{dL} = \frac{\alpha}{4\pi}\int_x^1 \frac{dy}{y}\left[p_{qq}(x/y)N_{q_i}(y, L) + p_{qg}(x/y)N_g(y, L)\right], \tag{5.3}$$

(x) - Hear first the four roots of all things.

$$\frac{dN_g(x,L)}{dL} = \frac{\alpha}{4\pi}\int_x^1 \frac{dy}{y}\left[p_{gg}(x/y)N_g(y,L) + p_{gq}(x/y)\sum_1^8 N_{q_i}(y,L)\right],$$

where

$$p_{qq}(y) = \frac{4}{3}\left[\frac{4}{(1-y)_+} - \delta(y-1) - 2 - 2y\right],$$

$$p_{gq}(y) = \frac{4}{3}\left[\frac{2(1-y)^2+2}{y}\right],$$

(5.4)

$$p_{qg}(y) = \frac{3}{16}\left[2(1-y)^2 + 2y^2\right],$$

$$p_{gg}(y) = 3\left[\frac{4}{(1-y)_+} + \frac{4}{y} + 4y(1-y)\right] - 2\delta(y-1),$$

$\frac{1}{(1-y)_+}$ is a distribution defined by:

$$\int_x^1 \frac{dy}{y}\frac{1}{(1-\frac{x}{y})_+}N(y) = \ln(1-x)N(x) + \int_x^1 \frac{dy}{y}\frac{1}{1-\frac{x}{y}}\left[N(y) - N(x)\right]. \quad (5.5)$$

The following consistency conditions are satisfied:

$$p_{qq}(y) = p_{gq}(1-y),$$

$$p_{qg}(y) = p_{qg}(1-y), \quad (5.6)$$

$$p_{gg}(y) = p_{gg}(1-y).$$

Eqs. (5.3-5.5) can be directly derived from the standard results of ref. (18-20) using the technique employed in ref. (21).

Higher orders in α have been neglected. σ_L/σ_T is of order α and is therefore asymptotically zero.

Let us try to use these formulae to compute the violations of the scaling law in deep inelastic scattering on nucleons.

Electron and neutrino deep inelastic scattering gives us very good information on the x distribution of quarks inside the nucleon, however no in

formation is available on the gluon distribution; we only know that gluons must be present in the nucleon: they carry about 0.48 of the total momentum. Unfortunately the theoretical predictions for scaling violations depend on the form of the gluon distribution. Two phenomena contribute to the scaling violations: firstly the shift of the quark and antiquark distributions due to gluon bremsstrahlung, secondly the creation of quark-antiquark pairs. Only the second process depends on the distribution of gluons. However it is quite reasonable that the sea will be negligible for x near to one ($x > 0.5$). Model independent conclusions can be reached only in this region.

If we want to be more quantitative we can try to put upper and lower bounds on the scaling violations using two extreme models of gluon distributions.

The first unreasonable possibility is that the gluons are concentrated at $x = 0$; $N_g(x, L) = 0.48\,\delta(x)/x$.

In this case the L derivative of the structure function is[21]:

$$(5.7)\qquad \frac{dF_2(x,Q^2)}{d\ln q^2} = \frac{\alpha(Q^2)}{3\pi}\left\{\left[3 + 4\ln(1-x)\right]F_2(x,Q^2) + x\int_x^1 dy\left[\left(-2\left(1+\frac{x}{y}\right) + \frac{4}{1-\frac{x}{y}}\right)F_2(y,Q^2) - \frac{4F_2(x,Q^2)}{1-\frac{x}{y}}\right]\right\}.$$

The value of the effective coupling constant $\alpha(Q^2)$ appears as a factor. Using as input[22]

$$(5.8)\qquad F_2^p(x) = (1-x)^3\left[1.274 + 0.5989(1-x) - 1.675(1-x)^2\right]$$

we obtain curve I of Fig. 6 for $\alpha(Q^2) = 0.4$. Notice that for such an high value of α corrections coming from the higher order terms may not be completely negligible. In this case we have neglected the gluon contribution which is positive: curve I is a lower bound on the derivative.

A physical motivated upper bound can be obtained supposing that the gluon distribution is proportional to the quark distribution in the region x near to one: for example we can assume that the x distribution is exactly $1.92(1-x)^3/x$. In this case one obtains the curve III of Fig. 6. In the region

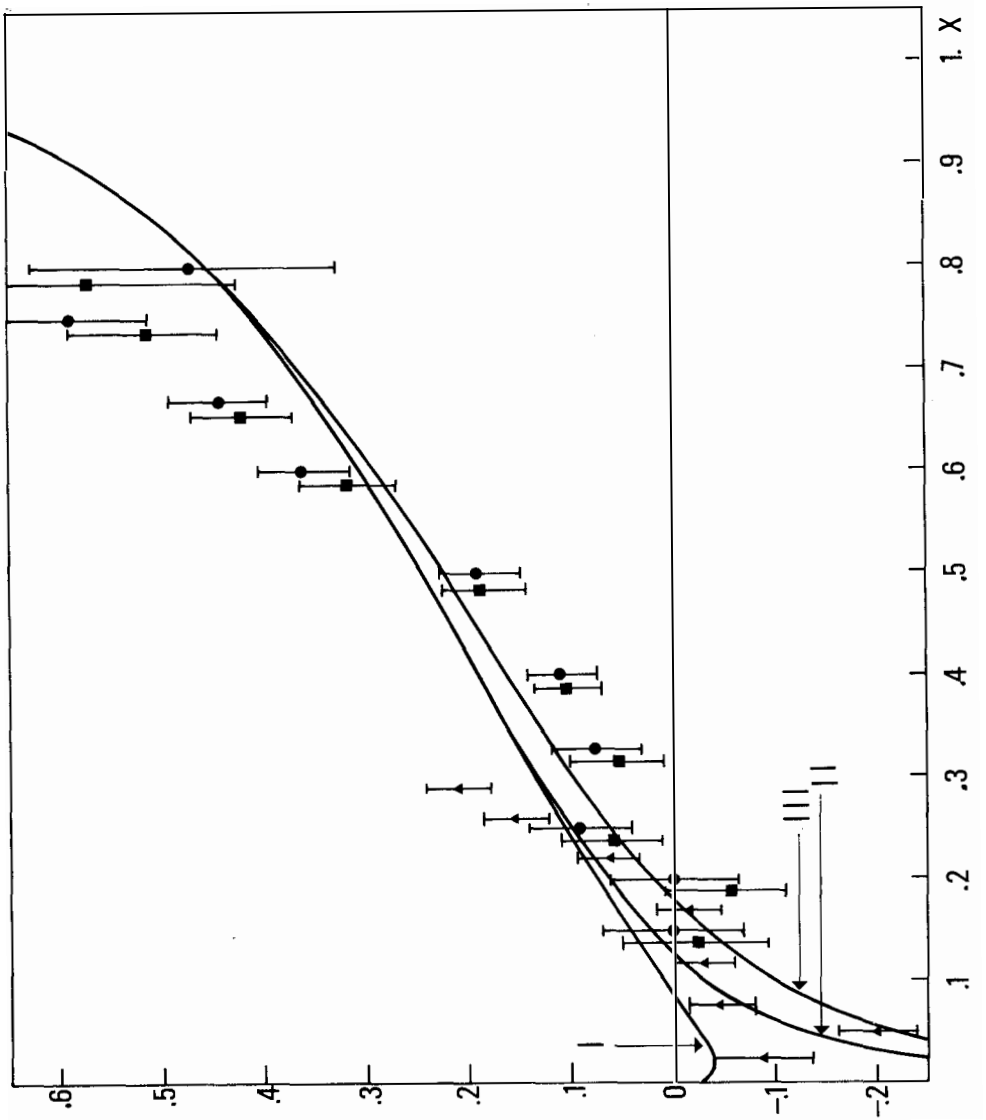

FIG. 6 - Curve I, II and III are respectively the predictions for $-\partial \ln F_2^p(x, Q^2)/\partial(\ln Q^2)$ assuming respectively, I the concentration of all gluons at $x = 0$, II an educated guess for the gluon distribution, and III a distribution $(1-x)^3$ for the gluons; the same predictions are obtained for the neutron with an accuracy of 0.02; $\alpha = 0.4$ has been assumed. (●) and (●) are respectively the experimental points for proton and deuterium[27]; (▲) are the experimental points for iron[28].

of large x there is no significant difference between the two curves for the two extreme choices of the gluon distribution. The difference is concentrated in the region of low x and it is due to the increase of the sea.

An educated guess for the gluon distribution can be obtained as follows: suppose that at a low value of L only p and n quarks are present in the proton. Using the master equation (5. 3) one can compute the quark, antiquark and gluon distributions for all values of L. If we impose the constraint that, at a particular value of L, the structure functions coincide with eq. (5. 8) we are able to fix the quark and gluon distributions at that particular L. Without entering into the details of how it can be done, we show directly the results: the predictions for the derivative of the structure functions are represented by curve II of Fig. 6.

A consistency check[2] of this model can be done comparing the predicted quark and antiquark distributions with the experimental data coming from neutrino and antineutrino scattering at Gargamelle. The agreement is not bad (see Fig. 7): notice that we have no free parameter and that we have used as input only data coming from deep inelastic electron scattering.

It seems to me that the predicted antiquark distribution is too concetrated near $x = 0$ (better data are needed to prove this conclusion); it is reasonable to suppose that the predicted gluon distribution has the same defect and that we are understimating the number of gluons in the large x region. My personal conclusion is that the correct prediction is between curve II and III. The ambiguity due to our ignorance of the gluon distribution is not large and sharp predictions can be made in the real asymptotic region.

Similar results can be obtained for the neutron structure functions. The difference among curves I, II and III for the neutron and the proton would hardly be observable in Fig. 6. It is always less than 0. 02.

These predictions are done in the region of very high Q^2 where $\alpha(Q^2)$ and M^2/Q^2 are small numbers. In the next section we shall see that in the intermediate Q^2 region where actual experiments are done, extra ambiguities are present which make the comparison between theory and experiments less straightforward.

6. - THE COMPARISON WITH EXPERIMENTS

ἁμαρτίης αἰτίη ἡ ἀμαθίη τοῦ χρέσσονος[x]
(Democritus)

When precise data on deep inelastic e-p scattering appeared in 1970 it was clear that violations of the Bjorken scaling were present[24]. These violations disappeared when the variable x' was used[25]; x and x' are asymptotically equal; the difference is only relevant at "low" values of Q^2. The amount and the very existence of scaling violations depends on the choice of the "correct" variable.

Up to now no strong theoretical argument has been found which allows a choice between x or x' or any other similar variable. However the choice of the "best" variable can be done using the experimental data plus a theoretical criterion of what we mean by the "best" variable.

In 1970 an experimental proof of Bjorken scaling was strongly desirable and the "best" variable was the one for which Bjorken scaling was better satisfied. In 1975 it was discovered that it is impossible to find a variable for which the Bjorken scaling law is satisfied both for proton and neutron deep inelastic scattering[26]. The experimental observation of scaling violations in the proton at fixed x' ($0.5 < x' < 0.7$) (see Fig. 8) suggests the use of a variable different from x', on the contrary the lack of scaling violations in the neutron at fixed x' would imply that x' is the "best" variable (see Fig. 9).

It is possible to use a new scaling variable x_{1975} for the proton and the old x' for the neutron, and this may be a simple phenomenological way to summarize the data. I think that it would be quite hard to find a theoretical justification in the framework of the parton model for the use of two different scaling variables: the criterion that the "best" variable must minimize the violations of Bjorken scaling, has led us to a dead end.

A new criterion is needed: we propose that the best variable should be such that scaling violations are the same for the neutron and the proton, at least in the large x region. If we use the experimental data[27,28] to com-

---

(x) - The cause of errors is ignorance of better.

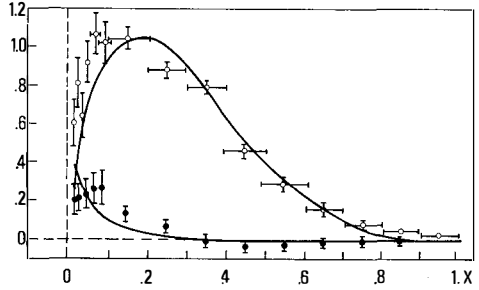

FIG. 7 -Our predictions for the amount of quarks (♦) and antiquarks (♦) in an isospin zero target are presented together with the experimental values extracted from neutrino and antineutrino scattering[23].

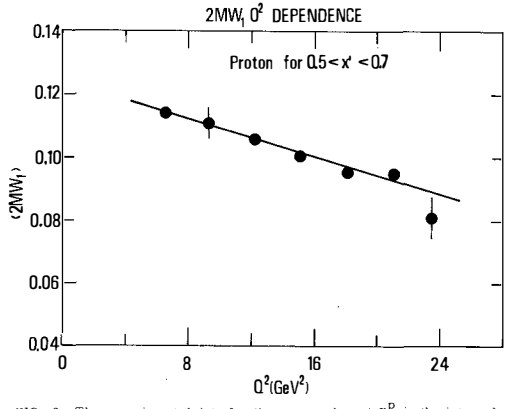

FIG. 8 - The experimental data for the mean value of F_1^p in the interval $0.5 \leq x' \leq 0.7$ plotted against Q^2.

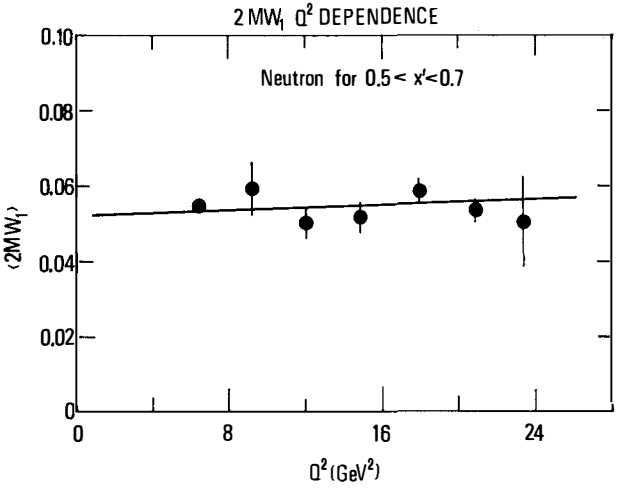

FIG. 9 - The experimental data for the mean value of F_1^n in the interval $0.5 \leq x' \leq 0.7$ plotted against Q^2.

pute the logaritmic derivative of the proton and of the neutron structure functions at fixed x, we find that they are roughly equal (see Fig. 6).

How is it possible that the two logaritmic derivatives at fixed x are equal and those at fixed x' are different? The answer can be easily found using the identity:

$$\left.\frac{\partial \ln F}{\partial Q^2}\right|_{x'} = \left.\frac{\partial \ln F}{\partial Q^2}\right|_{x} + \left.\frac{\partial \ln F}{\partial x}\right|_{Q^2} \cdot \left.\frac{\partial x}{\partial Q^2}\right|_{x'} . \tag{6.1}$$

In the x region we are interested in, one find that:

$$\frac{\partial \ln F_2^n}{\partial x} \simeq 1.2 \frac{\partial \ln F_2^p}{\partial x} . \tag{6.2}$$

Any change of variable modifies the Q^2 derivative of the neutron data more strongly than the proton data.

The variable x (and not x') satisfies the new criterion we have proposed, and we are going to use it in the rest of the paper (see Fig. 6). We stress that, if our intuition is wrong and if the predicted scaling violations must be compared with the derivative of the experimental data at fixed x', the present experimental evidence excludes that the observed scaling violations come from the mechanism described in this paper. However the data are not accurate enough to fix unambigously which is the best variable: any variable not too far from x would also satisfy our criterion within the experimental errors. The problem of the best variable arises from the existence of scaling violations due to the finite mass of the nucleons and of the quarks; these violations disappear asymptotically, however in the low Q^2 region it is impossible to disentangle the scaling violations which die as Q^2 is increased, from those which survive in the limit $Q^2 \to \infty$. The theory of these mass dependent scaling violations is practically lacking: the situation can be clarified in the framework of the so called covariant parton model of Landshoff and Polkingorne[29], unfortunately the analysis has not been carried out in detail.

Another problem is present: our asymptotic predictions do not distinguish among F_1 and F_2 (σ_L is asymptotically zero), however at present energies the logaritmic derivative of F_1 is systematically larger than that

of F_2 [27, 30]. Now it is not clear which function should be compared with the theoretical predictions: the chosen function must satisfy the requirement of minimizing the scaling violations due to finite mass effects.

The observed Q^2 dependence of the function F_2 can be well fitted using $\alpha = 0.4$ (see Fig. 6); a similar agreement between theory and experiment would be obtained using F_1 instead of F_2: in this case we would get $\alpha = 0.5$.

I would like to conclude that the observed scaling violations can be accounted for by interactions among partons with a coupling constant of order 0.4 - 0.5 in the few GeV^2 range. However there is still another effect which increases the error on the value of α: the large value of the coupling constant changes rather drastically with Q^2. The data in the central x region have $\langle Q^2 \rangle$ 3-6 GeV^2, while the data at x near to 1 have $\langle Q^2 \rangle$ 8-12 GeV^2.

In principle changing Q^2, we should also change the value of the effective coupling constant; in this particular instance this is not true because we are changing both Q^2 and x together. The effect we are talking about, is of the same order of magnitude as the neglected terms proportional to α^2 in the transition probabilities p (eq. (5.4)). We must realize that eq. (5.3) is asymptotically correct also if we substitute $\alpha(Q^2)$ by $\alpha(Q^2/(1-x))$; eq. (5.1) implies:

$$\alpha(Q^2/(1-x)) \simeq \alpha(Q^2) - \frac{25}{12\pi} \ln(1-x)\, \alpha^2(Q^2) \quad . \tag{6.3}$$

The difference is of order α^2. Notice that $\langle (1-x)Q^2 \rangle$ is roughly constant in a wide x region in the SLAC sample.

The effect of the neglected second order terms has not been computed at the present moment; it can be easily be of order of 30%, expecially in the region $x \sim 1$ where higher order contributions are expected to be enhanced. Terms proportional to α^2 are not negligible because our preferred value for the coupling constant is not small; they will distort the theoretical predictions in the region $x \sim 1$ and they will also change the Q^2 dependence of the moments of the structure function for N very large.

In our theoretical predictions we have also neglected the effect of the Q^2 dependence of the r. h. s. of eq. (5.7); the error we have introduced is

rather small and can be easily corrected using the data themselves and not their scaling fit (5. 8) in the r. h. s. of eq. (5. 7).

If I take care of all these ambiguities, I would estimate:

$$0.25 \leq \alpha(6\ \mathrm{GeV}^2) \leq 0.5 \,. \tag{6.4}$$

Correspondly:

$$0.4 \leq \alpha(1\ \mathrm{GeV}^2) \leq 1.2 \,. \tag{6.5}$$

The determination of the value of α is based mainly on the SLAC data. If high quality data coming from an high energy μ beam becomes available in the future for a large interval of Q^2, the determination of α can be improved. I hope that at that time the theoretical ambiguities will be solved: the transition probabilities will be computed at order α^2 and the scaling violations due to the finite mass of the proton will be understood.

7. - SCALING VIOLATIONS AND THE SEARCH FOR CHARM

The parton model gives rather interesting predictions when it is applied to neutrino and antineutrino induced reactions. In this paper we concentrate our analysis on the charged current processes; a similar analysis can be done for the case of neutral currents. If only V-A currents are present, we find:

$$\sigma_\nu = \frac{2G^2 M E_\nu}{\pi}\left[M_q^\nu + \frac{1}{3}M_{\bar{q}}^\nu\right], \quad \sigma_{\bar{\nu}} = \frac{2G^2 M E_{\bar{\nu}}}{\pi}\left[M_{\bar{q}}^{\bar{\nu}} + \frac{1}{3}M_q^{\bar{\nu}}\right] \tag{7.1}$$

$$\langle y\rangle_\nu = \frac{1}{2}\,\frac{6M_q^\nu + M_{\bar{q}}^\nu}{6M_q^\nu + 2M_{\bar{q}}^\nu}, \qquad \langle y\rangle_{\bar{\nu}} = \frac{1}{4}\,\frac{M_q^{\bar{\nu}} + 6M_{\bar{q}}^{\bar{\nu}}}{M_q^{\bar{\nu}} + 3M_{\bar{q}}^{\bar{\nu}}},$$

where σ denotes total cross section and y is the ratio between the neutrino (the antineutrino) energy and the energy given to the hadron system E_h: $y = E_h/E^\nu$. M_q^ν and $M_{\bar{q}}^\nu$ ($M_q^{\bar{\nu}}$ and $M_{\bar{q}}^{\bar{\nu}}$) are respectively the effective momentum carried by the quarks and the antiquarks which interact with the neutrino (with the antineutrino).

In the 4 quark model different results hold below and above the threshold for creation of charmed particles in the final state; below threshold

we find:

$$(7.2)\qquad M_q^{\nu} = \cos^2\theta_c M_n^2 + \sin^2\theta_c M_{\lambda}^2 \ , \qquad M_q^{\bar{\nu}} = M_p^2 \ ,$$

$$M_{\bar{q}}^{\bar{\nu}} = \cos^2\theta_c M_{\bar{n}}^2 + \sin^2\theta_c M_{\bar{\lambda}}^2 \ , \qquad M_{\bar{q}}^{\nu} = M_{\bar{p}}^2 \ .$$

Above threshold, transitions involving the p' quark are switched on:

$$(7.3)\qquad M_q^{\nu} = M_n^2 + M_{\lambda}^2 \ , \qquad M_q^{\bar{\nu}} = M_p^2 + M_{p'}^2 \ ,$$

$$M_{\bar{q}}^{\bar{\nu}} = M_{\bar{n}}^2 + M_{\bar{\lambda}}^2 \ , \qquad M_{\bar{q}}^{\nu} = M_{\bar{p}}^2 + M_{\bar{p}'}^2 \ .$$

It is commonly assumed that the quark distributions inside the nucleon can be divided into a valence contribution, an SU(3) symmetric sea of quarks and antiquarks and a charmed sea. If the target has isospin zero we get:

$$(7.4)\qquad M_p^2 = \frac{V^2}{2} + S^2 \ , \quad M_n^2 = \frac{V^2}{2} + S^2 \ , \quad M_{\lambda}^2 = S^2 \ , \quad M_{p'}^2 = C^2 \ ,$$

$$M_{\bar{p}}^2 = S^2 \ , \qquad M_{\bar{n}}^2 = S^2 \ , \qquad M_{\bar{\lambda}}^2 = S^2 \ , \quad M_{\bar{p}'}^2 = C^2 \ .$$

If we neglect the sea, no antiquarks are present in the nucleon: the antineutrino over neutrino total cross section ratio is below threshold:

$$(7.5)\qquad R \equiv \sigma_{\bar{\nu}}/\sigma_{\nu} = 1/3\cos^2\theta_c \simeq 0.35 \ .$$

At Gargamelle energies $R = 0.39$[23]; only a small contamination of antiquarks is present in the nucleon at low energy. The x distributions of quarks and antiquarks are shown in Fig. 7: the mean value of x of antiquarks ($\langle x_S \rangle$) is much smaller than that of the valence quarks ($\langle x_V \rangle$). The data suggests that at $Q^2 = 1\ \mathrm{GeV}^2$ (the mean value of Q^2 in the Gargamelle experiment is about $1\ \mathrm{GeV}^2$) the following relations hold:

$$(7.6)\qquad V^2 = 0.46 \ , \quad S^2 = 0.01 \ , \quad C^2 = 0 \ , \quad G^2 = 0.48 \ .$$

Obviously the data give no information about the amount of charmed quarks present in the proton; for simplicity I have assumed that the charmed

component of the proton can be neglected in the low Q^2 region. The conser vation of the total momentum implies the sum rule

$$V^2 + 6\,S^2 + 2\,C^2 + G^2 = 1 \quad , \tag{7.7}$$

which has been used to fix the momentum carried by the gluons (G^2).

Violations of the Bjorken scaling law are due to the presence of a threshold for charm production and to the Q^2 dependence of the quark distri butions. The first effect is characteristic of neutrino scattering. It will be shown here that both effects are needed to explain the observed violations of the scaling law in neutrino deep inelastic scattering: in the framework of the 4 quark model it is not simple to fit the experimental data neglecting the Q^2 dependence of the parton distributions.

The Q^2 dependence of the momentum carried by each component of the proton can be easily computed: proceeding as in section 3 we can derive from eqs. (5.3-4) an equation having the same form as eq. (3.20); its solution is[3]:

$$\begin{aligned}
V^2(Q^2) &= B_8\, G^{-32/75} \quad , \\
S^2(Q^2) &= \frac{3}{56} + \frac{1}{14} B_o G^{-56/75} + \left(\frac{1}{24} B_{15} - \frac{1}{6} B_8\right) G^{-32/75} \quad , \\
C^2(Q^2) &= \frac{3}{56} + \frac{1}{14} B_o G^{-56/75} - \frac{1}{8} B_{15} G^{-32/75} \quad , \\
G^2(Q^2) &= \frac{4}{7} - \frac{4}{7} B_o G^{-56/75} \quad ,
\end{aligned} \tag{7.8}$$

where

$$G(Q^2) = 1 + \frac{25}{12\pi}\, \alpha(\mu^2) \ln Q^2/\mu^2 \quad . \tag{7.9}$$

The constants B_o, B_8 and B_{15} can be fixed by requiring that eq. (7.6) be satisfied at $Q^2 = 1\ \mathrm{GeV}^2$.

In Fig. 10 the results have been plotted for $\alpha(1) = 0.5$, as functions of Q^2. Since G is a slowly varying function of Q^2 we can compute G from an effective Q^2 value

$$Q^2_{Eff} = 2\,M\,E\,\langle xy \rangle \quad , \tag{7.10}$$

where $\langle xy \rangle$ is the average value of xy, which is different for neutrino and antineutrino. At fixed energy E neutrino data involve larger value of

Q^2_{Eff} than antineutrino data.

Our predictions for the momentum carried by the charmed quarks must be taken cum grano salis: the effects of the large mass of the charmed quarks has not been taken into account. A more precise analysis would be needed to study effects that depend crucially on the amount of charmed quarks in the proton.

The cross sections and the y distribution below and much above the threshold for charm production can be easily computed.

The effects of the threshold may be simulated by a simple θ function in the mass W of the produced hadronic system:

$$\sigma_T(x,y) \simeq \sigma_B(x,y) + \sigma_C(x,y)\,\theta(W - W_T) \quad , \tag{7.11}$$

where σ_B is the cross section below the threshold for charm production, σ_C is the asymptotic cross section for producing a charmed final state and W_T is an effective threshold mass. Simple kinematical arguments, due to Barnett, suggest that:

$$W_T^2 = m_{p'}^2/\langle x \rangle \quad , \tag{7.12}$$

where $m_{p'}$ is the mass of the charmed quark and $\langle x \rangle$ is the mean value x of the quarks from which the p' is produced. Charm is produced by neutrinos mainly out of valence quarks, by antineutrinos out of sea quarks. Using $m_{p'} = 2$ GeV, $\langle x_V \rangle = 0.25$ and $\langle x_S \rangle = 0.13$ we estimate:

$$W_T^{\nu} \simeq 4 \text{ GeV} \quad , \qquad W_T^{\bar{\nu}} \simeq 5.5 \text{ GeV} \quad . \tag{7.13}$$

The higher value of the effective threshold for antineutrino is caused by the exoticity of the hadronic final state (B = 1, C = -1).

In Figs. 11 and 12 we show our predictions for $\langle y \rangle_{\nu}$ and R respectively for various values of W_T and a. The data for $\langle y \rangle_{\bar{\nu}}$ come from the HPWF collaboration. For simplicity the same threshold has been used for neutrino and antineutrino.

When $a = 0$ the scaling violations due to the strong interactions are absent and when $W_T = \infty$ the charm threshold never opens. It is apparent that both $a \neq 0$ and $W_T < \infty$ are needed to fit the data for $\langle y \rangle_{\bar{\nu}}$; in this

case R is predicted to rise with E. If the momentum carried by each quark were Q^2 independent, R would stay almost constant and be insensitive to the charm threshold; in fact the increased proportion of momentum carried by the sea makes R to behave as in Fig. 12. While this prediction is not supported by the published data of the Caltech group[32] (although not excluded within quoted errors) a sharp rise of R has been reported by the HPWF group[33, 34].

In the infinite energy limit very simple predictions are obtained:

$$(7.14) \qquad \sigma_\nu = \sigma_{\bar\nu} = \frac{G^2 M E}{\pi} \frac{2}{7} \quad , \qquad \langle y \rangle_\nu = \langle y \rangle_{\bar\nu} = \frac{7}{16} \quad .$$

If scaling violations were absent, eq. (7.6) implies that the fraction $\Delta\sigma/\sigma$ of charmed final states would not exceed 10% even at infinite energy. The predictions with scaling violations included are shown in Fig. 13. If charmed particle have an average branching ratio into muons of the order of 5% to 10%, the observed yield of events with muons of opposite charge is obtained[35, 36].

Dimuons with equal charge[35] may come from the production of a charmed quark-antiquark pair in an event with $\Delta C = 0$. A very rough estimate of the order of magnitude of the cross section for the creation of two charmed particles is:

$$(7.15) \qquad \sigma_{C\bar C} \simeq C^2 \sigma_T \quad .$$

A careful study of the effects due to the high p' mass would be needed to understand if this mechanism may explain the observed yield of equal sign dimuons. It is also possible that the equal sign dimuons come from the decay of a massive b quark[37] produced out of a p' quark.

A distinctive feature of the scaling violations due to the strong interaction is that the x distributions of quarks and antiquarks shift toward zero with increasing Q^2. This effect has been observed in electroproduction and should also be observed in neutrino production. Predictions for the behaviour of the structure functions at fixed x can be made using the same techniques as in section 5. However it may be convenient to concentrate on global quantities such as $\langle x \rangle$.

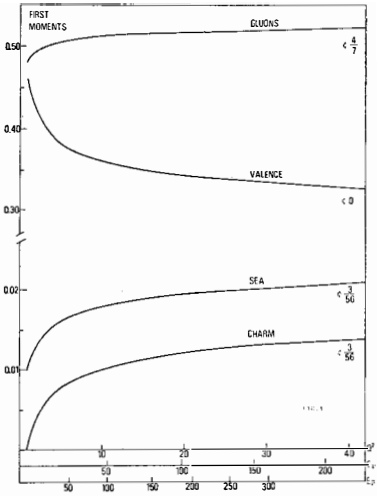

FIG. 10 - Momenta carried by the gluons, the valence quarks, the SU(3) symmetric sea and the charmed sea. The arrows indicate the asymptotic values. $G + 2V + 6G + 2C = 1$ is identically satisfied. The curves have been computed using $\alpha(1\ GeV^2) = \alpha = 0.5$.

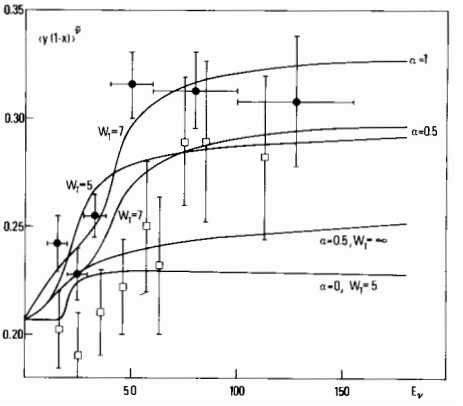

FIG. 11 - Average value of $y_{\bar{\nu}}$ for different values of α and W_T, the effective invariant mass for charm threshold. $\alpha = 0$ corresponds to Q^2 independent parton distributions. $W_T \to \infty$ corresponds to neglecting effects for charm production. Both effects seem to be needed to reproduce the data. α is the coupling constant at $Q^2 = 1\ GeV^2$. The experimental points are taken from ref. (31).

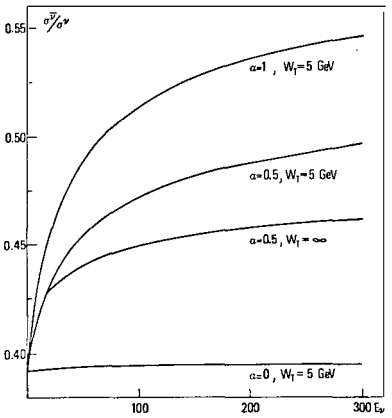

FIG. 12 - The ratio $\sigma^{\bar{\nu}}/\sigma_{\nu}$ for different values of $\alpha(1\ \mathrm{GeV}^2)$ and W_T, the effective invariant mass for charm threshold.

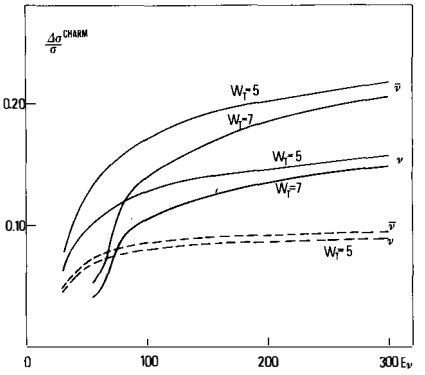

FIG. 13 - The prediction for the fraction $\Delta\sigma/\sigma$ of charmed final states for neutrino and antineutrino. The dashed line is obtained with Q^2 independent parton distributions, the full lines are obtained assuming $\alpha = 0.5$ at $Q^2 = 1\ \mathrm{GeV}^2$; W_T is the effective invariant mass for charm production.

Evolution equations like eq. (7. 8) can be written also in this case[3]. This problem will not be studied here: the interested reader can find a careful treatment of this and of many other phenomena concerning scaling violations in neutrino scattering in the paper of Altarelli presented at this Rencontre de Moriond[38].

8. - CONCLUSIONS

In this paper we have shown that in relativistic quantum field theory the breaking of the Bjorken scaling law can be understood in terms of successive fragmentations of the partons. The parton model relations among electron, neutrino and antineutrino scattering are preserved, provided we use Q^2 dependent parton distributions.

The scaling violations observed in deep inelastic electron scattering can be understood using a strong interaction coupling constant of the order 0. 4 in the few GeV range. Using this value for the strong interaction coupling constant we compute the scaling violations in neutrino and antineutrino scattering. The most interesting prediction is a large increase in the momentum carried by the sea of antiquarks with increasing energy. The mean value of y in antineutrino scattering and the ratio of the total antineutrino and neutrino cross sections are consequently affected. Without this effect it is hard to understand the present experimental data in the framework of the 4 quark model. It appears that a correct treatment of the violations of the Bjorken scaling law is a necessary ingredient in any successfully analysis of neutrino scattering at present energies.

The author is really grateful to R. K. Ellis for a critical reading of the manuscript.

REFERENCES

(1) - G. Parisi and R. Petronzio, A dynamical approach to deep inelastic scattering, Rome preprint 617 (1975); to be published on Nuovo Cimento.

(2) - G. Parisi and R. Petronzio, On the breaking of Bjorken scaling, Rome preprint; submitted to Physics Letters B.

(3) - G. Altarelli, G. Parisi and A. Petronzio, Charmed quarks and asymptotic freedom in neutrino scattering, Rome preprint, submitted to Physics Letters B.

(4) - A. M. Poliakov, Sov. Phys. -JEPT 32, 296 (1971).

(5) - J. Kogut and L. Susskind, Phys. Rev. D9, 697 (1971).

(6) - S. D. Drell, D. J. Levy and T. M. Yan, Phys. Rev. 187, 2159 (1970).

(7) - We use the same notation as G. Altarelli, Riv. Nuovo Cimento 4, 335 (1974).

(8) - G. Parisi, Phys. Letters 42B, 114 (1972).

(9) - G. Parisi, Serious difficulties with canonical dimensions, Frascati report LNF-72/94 (1972).

(10) - N. Cabibbo and M. Rocca, CERN preprint Th 1974.

(11) - N. Cabibbo and G. Parisi (unpublished).

(12) - D. Bailin, A. Love and D. V. Nanopoulos, Lett. Nuovo Cimento 9, 501 (1974).

(13) - K. Symanzik, Lett. Nuovo Cimento 6, 420 (1973).

(14) - S. L. Glashow, J. Iliopoulos and L. Maiani, Phys. Rev. D2, 1285 (1970).

(15) - G. 't Hooft, Marseille Conference 1972 (unpublished).

(16) - H. D. Politzer, Phys. Rev. Letters 30, 1346 (1973).

(17) - D. J. Gross and W. Wilzek, Phys. Rev. Letters 30, 1343 (1973).

(18) - H. Georgi and H. D. Politzer, Phys. Rev. D9, 416 (1974).

(19) - D. J. Gross and W. Wilczek, Phys. Rev. D9, 980 (1974).

(20) - A. Zee, F. Wilzeck and S. L. Treiman, Phys. Rev. D10, 2881 (1974).

(21) - G. Parisi, Phys. Letters 43B, 207 (1973); 50B, 367 (1974).

(22) - G. Miller et al., Phys. Rev. D5, 528 (1972).

(23) - CERN-Gargamelle collaboration, Phys. Letters 46B, 274 (1973).

(24) - D. Wilson, Review talk presented at the Kiev Conference (1970).

(25) - E. D. Bloom and F. J. Gilman, Phys. Rev. Letters 25, 1140 (1970).

(26) - R. Taylor, Review talk presented at the Stanford Conference (1975).

(27) - A. Bodek et al., SLAC Publ. 1445 (1975).

(28) - C. Chang et al., Phys. Rev. Letters 35, 901 (1975).

(29) - N. Cabibbo, G. Parisi, M. Testa and A. Verganelakis, Lett. Nuovo Cimento 4, 569 (1970).

(30) - E. M. Riordan, Phys. Letters 52B, 249 (1973).

(31) - A. Benvenuti et al., Further data on the high-y anomaly in inelastic antineutrino scattering, Preprint HPWF 76/1 (1976).

(32) - B. C. Barish et al., Phys. Rev. Letters 35, 1316 (1975).

(33) - A. K. Mann, Talk presented at this Rencontre.

(34) - C. Rubbia, Talk presented at this Rencontre.

(35) - A. Benvenuti et al., Phys. Rev. Letters 35, 1199, 1203 and 1249 (1975).

(36) - B. G. Barish et al., Cal. Tech. Report 58-485 and 68-510 (1975).

(37) - H. Harari, SLAC-Pub-1589 (1975).

(38) - G. Altarelli, Talk presented at this Rencontre.